



## Resistive switching in nanostructured thin films

H. Silva, H. L. Gomes, Yu. G. Pogorelov, P. Stallinga, D. M. de Leeuw, J. P. Araujo, J. B. Sousa, S. C. J. Meskers, G. Kakazei, S. Cardoso, and P. P. Freitas

Citation: *Applied Physics Letters* **94**, 202107 (2009); doi: 10.1063/1.3134484

View online: <http://dx.doi.org/10.1063/1.3134484>

View Table of Contents: <http://scitation.aip.org/content/aip/journal/apl/94/20?ver=pdfcov>

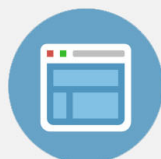
Published by the [AIP Publishing](#)

---



## Re-register for Table of Content Alerts

Create a profile.



Sign up today!



## Resistive switching in nanostructured thin films

H. Silva,<sup>1,2</sup> H. L. Gomes,<sup>1,a)</sup> Yu. G. Pogorelov,<sup>2</sup> P. Stallinga,<sup>1</sup> D. M. de Leeuw,<sup>3</sup>  
J. P. Araujo,<sup>2</sup> J. B. Sousa,<sup>2</sup> S. C. J. Meskers,<sup>4</sup> G. Kakazei,<sup>2</sup> S. Cardoso,<sup>5</sup> and P. P. Freitas<sup>5</sup>

<sup>1</sup>Center of Electronics Optoelectronics and Telecommunications (CEOT), Universidade do Algarve, Campus de Gambelas, 8005-139 Faro, Portugal

<sup>2</sup>Departamento de Física, Faculdade de Ciências, IFIMUP and IN-Institute of Nanoscience and Nanotechnology, Universidade do Porto, Rua do Campo Alegre 687, 4169-007 Porto, Portugal

<sup>3</sup>Philips Research Laboratories, Professor Holstlaan 4, 5656 AA Eindhoven, The Netherlands

<sup>4</sup>Molecular Materials and Nanosystems, Eindhoven University of Technology, P.O. Box 513, 5600 MB Eindhoven, The Netherlands

<sup>5</sup>INESC-MN and IN-Institute of Nanoscience and Nanotechnology, Rua Alves Redol 9-1, 1000-029, Lisboa, Portugal

(Received 10 February 2009; accepted 16 April 2009; published online 20 May 2009)

Planar capacitor structures based on granular films composed of nanometric ferromagnetic grains embedded in an insulating  $\text{Al}_2\text{O}_3$  matrix can switch between a high-conductance and a low-conductance state. The switching properties are induced by a forming process. The ON/OFF resistance ratio is as high as  $10^4$  under an electrical field of only 15 kV/m. This resistive switching is accompanied by a capacitive switching between two well-defined voltage-independent states, a behavior that is not readily explained by the filamentary type of conduction. © 2009 American Institute of Physics. [DOI: 10.1063/1.3134484]

Nanometer-scale magnetic materials are gaining widespread interest because of interesting effects arising from the reduction of their size. Among these, structures consisting of magnetic single-domain nanoparticles are a class of granular magnetoresistive films interesting for magnetic sensors and magnetic data storage devices.<sup>1,2</sup> In this work we show that these same granular structures also have interesting electrical switching properties, making them also highly attractive for applications in resistance random-access memories. Furthermore, this work thus also draws attention to the fact that the use of these granular materials in magnetic devices should also take their electrical resistive-switching properties into account.

Electrical switching is a remarkably universal phenomenon in composite systems, in which metal nanoparticles are embedded in an insulating or semiconducting host. In spite of the numerous studies,<sup>3-9</sup> the memory mechanism is still elusive. This work reveals some interesting features, which may help to better understand the physics behind resistive switching. In summary, it is shown that (i) the so-called negative differential resistance region often observed in the current-voltage characteristics of memory devices is unusual in these structures and consists of a single abrupt switching event and that (ii) the impedance data reveal that there are only two capacitance states involved in the resistive switching, showing that switching is between two well-defined discrete states.

The thin films were deposited on glass substrates using Xe-ion beam sputtering acting alternately on two separate targets. This procedure has been described elsewhere.<sup>10</sup> Alumina was sputtered from an  $\text{Al}_2\text{O}_3$  target plate, and  $\text{Co}_{80}\text{Fe}_{20}$  was sputtered from a mosaic target (pieces of Fe on a Co plate). The base pressure during sputtering was  $8 \times 10^{-8}$  Torr. The films were fabricated from alternating

$\text{Al}_2\text{O}_3$  (30 Å) and  $\text{CoFe}$  (9 Å) layers (see Fig. 1). Structures with ten such layers were measured. Gold electrodes approximately 3 mm long, 500  $\mu\text{m}$  wide, and 100 nm thick and separated by a gap ( $L$ ) of 100  $\mu\text{m}$  were deposited on top by thermal evaporation through a shadow mask. Current-voltage ( $I$ - $V$ ) characteristics were measured using a Keithley 6487 picometer-voltage source, and the capacitance-voltage plots were measured with a Fluke PM 6306 RCL meter.

Initially, the thin films behave as insulating materials. The current-voltage ( $I$ - $V$ ) characteristics were measured by scanning the applied voltage from 0 V up to successively higher voltages. They exhibit a symmetrical behavior with a typical resistance of 1 G $\Omega$  and little hysteresis. This behavior is similar to the one represented in Fig. 2(a) for negative

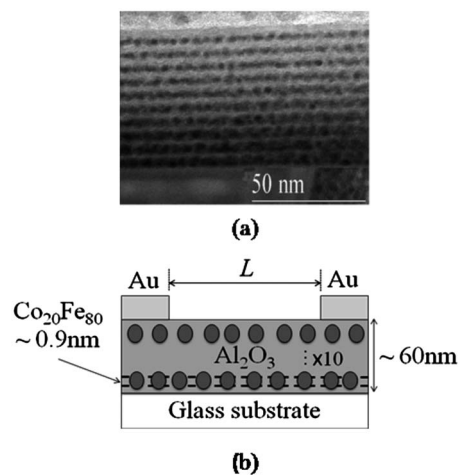


FIG. 1. (a) Transmission electron microscopy image of a ten-layer  $\text{Co}_{80}\text{Fe}_{20}$  film. The grains,  $\text{Co}_{80}\text{Fe}_{20}$  islands, are the dark spots with average lateral size of 5 nm and separated by thin dielectric layers of  $\text{Al}_2\text{O}_3$ . (b) Schematic of the physical structure. The gold electrodes have a length of 3 mm, width of 500  $\mu\text{m}$ , and height of 100 nm. They are separated by a gap ( $L$ ) of 100  $\mu\text{m}$ . The discontinuous layer of  $\text{Co}_{80}\text{Fe}_{20}$  is embedded in the  $\text{Al}_2\text{O}_3$  matrix typically 60–70 nm thick.

<sup>a)</sup>Author to whom correspondence should be addressed. Electronic mail: hgomes@ualg.pt.

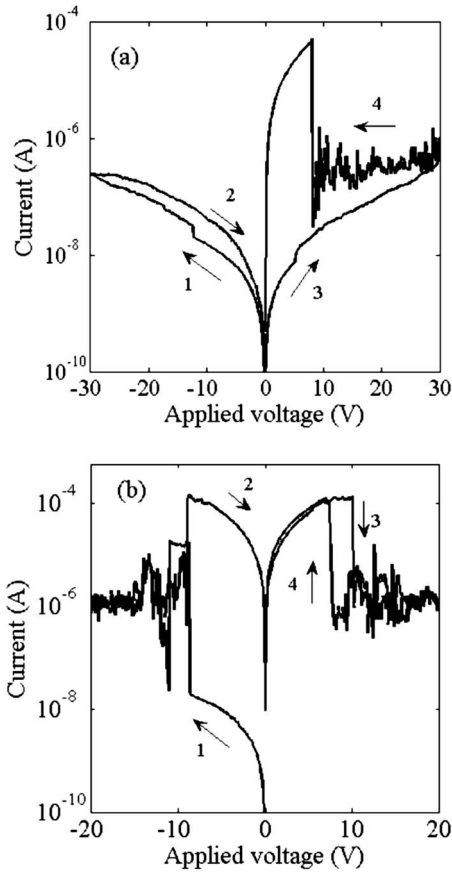


FIG. 2. (a) Current-voltage (*I-V*) plots showing a sudden and irreversible change (forming process). In the positive-bias return-voltage scan, the current becomes noisy and switches between a low-conductive and a high-conductive state at around 10 V. (b) *I-V* characteristics of a device obtained after forming.

bias. When the scanning voltage range was increased up to 30 V, the negative-bias region kept its normal behavior; however, in the return scan of the positive-bias sweep, an irregular behavior was observed. The current became very noisy and its average value is independent of voltage in the range of 30–10 V. Then, at 10 V, a switching event occurred which increased the current more than two orders of magnitude. After the switching to a high-conductive state, the noise in current also disappeared. The device *I-V* characteristics are now permanently modified and exhibit the behavior shown in Fig. 2(b). This change in the behavior after a stressing voltage is known as “forming” and is commonly reported for other memory devices.<sup>11–14</sup> According to the literature, this forming step involves the generation of oxygen-related defects by the high electric field. These defects can then be programmed by a voltage pulse and thus leads to a memory device.

Once the device is formed, the *I-V* characteristics can be programmed from a typical OFF state to an ON state. The ON-state up-scanning curve has a sudden downward jump at around 10 V, followed by a noisy behavior. This type of *I-V* characteristics resembles very much the negative differential resistance characteristics reported in the literature for other memory devices.<sup>14</sup> Reliable switching is now obtained by a voltage pulse below and above the sharp drop in current at the critical voltage of 10 V. For instance, switching from the low-conductive state to the high-conductive state is achieved by applying a voltage that is lower than 10 V. On the other

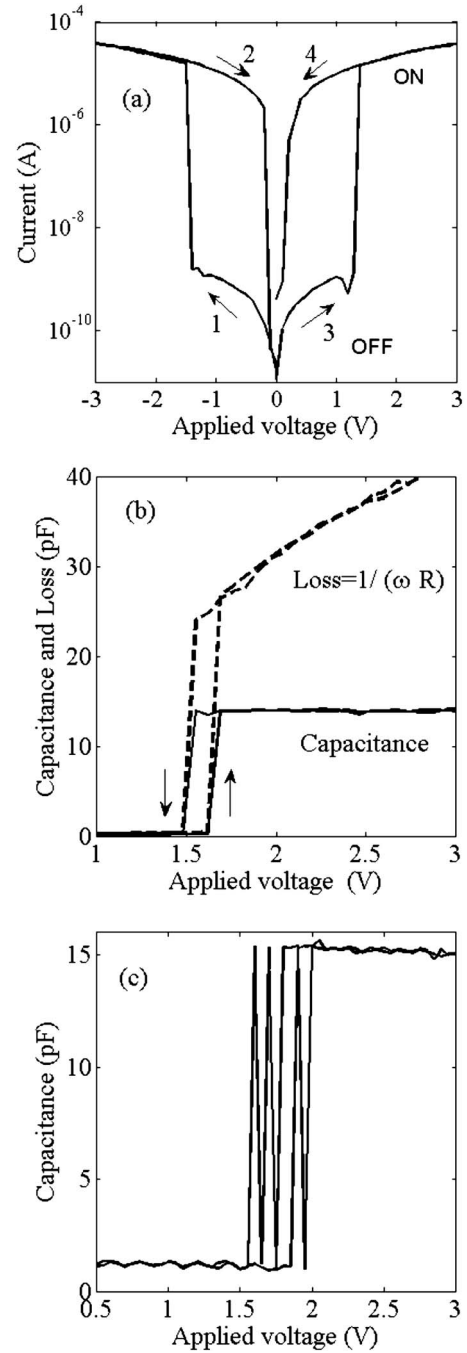


FIG. 3. (a) Low-bias region of the final bistable current-voltage characteristics observed after many ON/OFF cycles. (b) Step change in capacitance accompanying the resistive switching ( $f=1$  kHz). (c) Multiple capacitance jumps between two discrete states occurring at a constant voltage.

hand, a voltage pulse above the threshold voltage of 10 V must be applied to reset the device to the low-conductive state. This type of switching behavior is typical of many insulating oxides.<sup>3</sup>

The ON and OFF states are stable for periods of several days. It is possible that these retention times are even longer, but no detailed studies have been conducted, yet. However, in one of our devices we encountered an additional effect that might shine some light on the way the device functions. After many cycles between the ON and OFF states, the low-voltage range shows a different behavior, as shown in Fig. 3(a). Most interestingly, the switching to the ON state occurs now for lower biases. This type of switching is highly repro-

ducible, occurring always at exactly the same bias ( $V=1.5$  V). However, the retention time of the ON state is in a time scale of 1–3 min, and the device thus no longer behaves as nonvolatile memory.

Switching was also studied using small-signal impedance measurements. It was observed that resistive switching is accompanied by a single step change in a capacitance of 14 pF, as shown in Fig. 3(b). This change between two voltage-independent capacitance states indicates that there are only two discrete states of the sample. When scanning the voltage slowly, it is possible to observe a series of capacitance jumps between the low-capacitance and the high-capacitance state. These transitions are always located in a narrow voltage range, which coincides with the voltage where resistive switching occurs [see Fig. 3(c)].

Resistive switching is often attributed to the formation of filaments across the sample.<sup>3,15</sup> Indeed filaments have been observed in lateral structures of SrTiO<sub>2</sub> using local conducting atomic microscopy.<sup>15</sup> The authors proposed that a network of dislocations forms during the electroforming step, and filling and emptying of the dislocations with oxygen ions correspond to the OFF and ON switching. However, the observation here that the capacitance switches are systematically between well-defined initial and final values, even after repeated switching as shown in Fig. 3(c), seems counterintuitive in a filamentary type of conduction. It is implausible that for every switching event, the same exact number of identical filaments is formed. Also note that a single filament would be unable to carry the current observed (0.1 mA). Therefore, this observation of discrete capacitance states cannot be simply explained by a discrete filamentary type of conduction. We suggest that the increase in capacitance is caused by a trapping mechanism and an associated charge accumulation, which decreases the effective distance between the electrodes. Charges can be trapped in a matrix of defects that can be formed by the metallic grains. Once the traps are filled, charge neutrality must be maintained with opposite charges in their vicinity. If these compensating charges are mobile and located in the Al<sub>2</sub>O<sub>3</sub> matrix, they will increase the free carrier density and allow for much higher conductivity of the oxide. These charge accumulating regions surrounding the defects can grow and expand. Eventually, neighboring regions can merge together. When this occurs the effective distance between the electrodes is decreased and the internal electric field increases, thus accelerating the merging of these regions until charge carriers can easily travel from one electrode to another. The layer with nanoparticles becomes a conductive sheet, and the capacitance approximates that of two parallel plate capacitors, formed by the gold electrodes and the conductive layer, which is a huge increase. To exemplify this phenomenological model, we represent the sample by a network of  $N$  capacitors separated by a distance  $\Delta d$ , as shown in Fig. 4. The total applied field across a straight path is then  $E=V/N\Delta d$ , where  $V$  is the applied voltage. If two neighbor regions merge together, this is equivalent to a local electrical short, as shown in path 2 in Fig. 4. The electric field across this particular path rises to  $E=V/(N-N_{SC})\Delta d$ , where  $N_{SC}$  is the number of shorts. The higher electric field will favor the merging of more regions. Eventually, a cascade of connections will occur, which rapidly creates an array of conducting paths across the entire sample in an avalanche process.

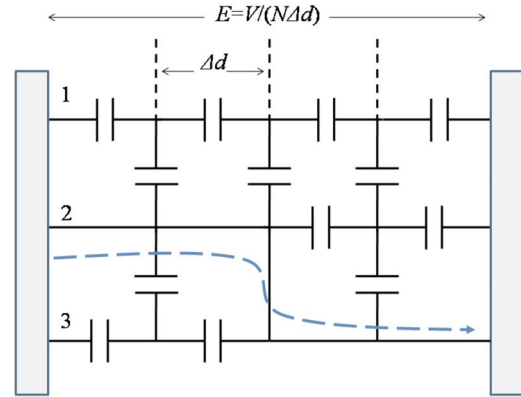


FIG. 4. (Color online) Phenomenological model to explain the formation of a network of conducting paths across the sample.

In conclusion, planar-type capacitor device structures, consisting of ferromagnetic grains embedded in an insulating Al<sub>2</sub>O<sub>3</sub> matrix, show a memory-type resistive-switching effect. The device has a large dynamic range of the resistance change. Most interestingly, the threshold voltage for switching is highly reproducible and corresponds to a weak programming field (15 kV/m), making these devices compatible with complementary metal-oxide semiconductor technology, an advantage for a realistic commercial device application. The discrete nature of capacitance switching presented here provides interesting information. While it is becoming accepted that switching is due to the establishment of discrete conducting filaments, the present results strongly suggest that, upon switching, there is also a charge trapping process in the device that causes a dramatic increase in the overall device capacitance. It is important to elucidate the role of these charges in the microscopic mechanism involved in the resistive switching.

This work was financially supported by the Fundação para a Ciência e Tecnologia (FCT) through Grant No. SFRH/BD/24190/2005 and the Center of Electronics Optoelectronics and Telecommunications (CEOT).

- <sup>1</sup>P. Sheng, B. Abeles, and Y. Aire, *Phys. Rev. Lett.* **31**, 44 (1973).
- <sup>2</sup>G. N. Kakazei, Yu. G. Pogorelov, A. M. L. Lopes, J. B. Sousa, P. P. Freitas, S. Cardoso, M. M. P. Azevedo, and E. Snoeck, *J. Appl. Phys.* **90**, 4044 (2001).
- <sup>3</sup>R. Waser and M. Aono, *Nature Mater.* **6**, 833 (2007).
- <sup>4</sup>M. J. Rozenberg, I. H. Inoue, and M. J. Sánchez, *Phys. Rev. Lett.* **92**, 178302 (2004).
- <sup>5</sup>A. Sawa, *Mater. Today* **11**, 28 (2008).
- <sup>6</sup>S. H. Chang, J. S. Lee, S. C. Chae, S. B. Lee, C. Liu, B. Kahug, and T. W. Noh, *Phys. Rev. Lett.* **102**, 026801 (2009).
- <sup>7</sup>J. C. Scott and L. D. Bozano, *Adv. Mater. (Weinheim, Ger.)* **19**, 1452 (2007).
- <sup>8</sup>L. D. Bozano, B. W. Kean, V. R. Deline, J. R. Salem, and J. C. Scott, *Appl. Phys. Lett.* **84**, 607 (2004).
- <sup>9</sup>L. P. Ma, S. M. Pyo, J. Y. Ouyang, Q. F. Yu, and Y. Yang, *Appl. Phys. Lett.* **82**, 1419 (2003).
- <sup>10</sup>G. N. Kakazei, P. P. Freitas, S. Cardoso, A. M. L. Lopes, Yu. G. Pogorelov, J. A. M. Santos, and J. B. Sousa, *IEEE Trans. Magn.* **35**, 2895 (1999).
- <sup>11</sup>J. G. Simmons and R. R. Verderber, *Proc. R. Soc. London, Ser. A* **301**, 77 (1967).
- <sup>12</sup>R. Blessing and H. Pagnia, *Thin Solid Films* **52**, 333 (1978).
- <sup>13</sup>F. Verbakel, S. C. J. Meskers, M. Cölle, M. Büchel, H. L. Gomes, R. A. J. Janssen, and D. M. de Leeuw, *Appl. Phys. Lett.* **91**, 192103 (2007).
- <sup>14</sup>A. Baikalov, Y. Q. Wang, B. Shen, B. Lorenz, S. Tsui, Y. Y. Sun, Y. Y. Xue, and C. W. Chu, *Appl. Phys. Lett.* **83**, 957 (2003).
- <sup>15</sup>K. Szot, W. Speier, G. Bihlmayer, and R. Waser, *Nature Mater.* **5**, 312 (2006).